Atomic-Force-Microscopy Observations of Tracks Induced by Swift Kr Ions in Mica

F. Thibaudau and J. Cousty
SPAS-DRECAM, Centre d'Etudes Nucléaires de Saclay, 91191 Gif-sur-Yvette CEDEX, France

E. Balanzat and S. Bouffard
Centre Interdisciplinaire de Recherches avec les Ions Lourds, BP 5133, rue Claude Bloch, 14040 Caen CEDEX, France
(Received 29 April 1991)

For the first time, latent tracks induced by swift Kr ions have been directly observed in mica. These tracks are imaged by atomic force microscopy as hollows which are associated with softer areas in the mica surface. The track core is formed by disordered mica. The mean diameter of the observed hollows increases with the electronic stopping power of the ions. The track shape along the ion path is deduced from the analysis of both the number of the tracks per unit area and their diameter distribution. These observations are the first images of nanometric changes of elastic properties.

PACS numbers: 61.80.Jh, 61.16.Di

Near-field microscopies, such as scanning tunneling microscopy (STM) or atomic force microscopy (AFM), allow direct observation of solid surfaces at the atomic scale. Thus, these new microscopies are well suited for the investigation of surface defects. In earlier STM experiments [1], defects in silicon surfaces bombarded by Ar^+ ions were observed. More recently, STM studies of defects due to ion impact in surfaces of graphite were reported [2,3]. The main defects observed were hillocks which have been associated with cascade collisions beneath the surface. These extended damages are produced by multiple collisions occurring during the slowing down of a primary knocked-out atom. For swift heavy ions a second mechanism dominates the energy loss: the interactions between the incoming projectile and the target electrons (electronic stopping power dE/dx_e). The transferred energy, which could reach values as high as a few tenths of a keV per nm, is highly localized around the ion path and could create extended defects. Numerous studies have been devoted to the description of the morphology of the ion tracks [4]. The most complete description has been carried out for magnetic oxides [5,6], where high-resolution transmission-electron-microscopy (HREM) observations show that the track morphology depends on the dE/dx_e value of the swift heavy ions. The tracks are described as continuous cylinders (with a diameter of about a few nanometers) of amorphous matter for high dE/dx_e. For low dE/dx_e, a chaplet of spherical damaged zones randomly distributed along the ion path is observed. Up to now, such a description is relevant for all the materials, irradiated by swift heavy ions, which can be observed by HREM. For materials where defects induced by ions fade during HREM experiments, only less direct observations are available. This is the case for organic compounds and mostly for inorganic insulators. Among these materials, mica has been the most extensively studied, by track etching experiments [7,8] and small-angle x-ray and neutron scattering [9,10]. However, the etching process may depend on several parameters which make the deduced description of the latent tracks hazardous. On the other hand, small-angle scattering is only sensitive to local changes in atomic or electronic density and not to the atomic arrangement. The shape of the diffracting object is roughly deduced: A chaplet of spheres and a cylinder give different signatures. Mean values of the atomic density in the track and of its radial extension are obtained. These values are, to some extent, model dependent.

In this Letter, we report the first direct observations, made by AFM, of tracks in muscovite mica irradiated by swift heavy ions. With AFM, a fine diamond probe tip fixed on a small spring is scanned over the sample surface. The spring deflects according to the force between the tip and the surface. In the constant-force mode, a feedback system adjusts the relative position of the tip and the surface so that the force remains constant. So, an AFM image generally reproduces the topography of the surface [11]. Moreover, local changes in the interaction between tip and surface or in the elastic response of the surface to the applied force cause some relief in the image.

The AFM used in these experiments was a commercially available model [12]. It was equipped with a small V-shaped cantilever in Si_3N_4. The image was obtained with a contact mode between tip and surface. This force was in the 10^{-8}-N range. The irradiations were performed at the GANIL cyclotron accelerator (Caen) with 34.5-MeV/amu ^{84}Kr ions. The ion beam hit a stack of 40-μm-thick mica sheets. The ion energies and their stopping power are given in Table I for the different samples studied.

Prior to AFM investigation, the mica was cleaved by means of an adhesive tape. AFM images of unirradiated mica show a large area (800×800 nm^2) without defects on which one can observe a hexagonal lattice with a bump-to-bump distance of 0.52 nm, in agreement with previous measurements [13]. These images do not show the atomic arrangement of the mica surface. However,

TABLE I. Values of the ^{84}Kr-ion energy at the input and the output of each sheet studied. The mean electronic stopping power dE/dx_e is also reported, with the corresponding measured radius of the hollow.

Input energy (MeV/amu)	Output energy (MeV/amu)	Mean electronic stopping power (MeV mg^{-1}cm^2)	Measured radius of the hollow (nm)
34.5	32.3	16.3	<1
32.3	30.0	17	<1
24.6	21.8	20.55	3 ± 0.5
15.6	11.9	27.52	4 ± 1
7.6	2.18	40.2	5.5 ± 1

such a resolution is sufficient for our purpose. The AFM images of irradiated mica depend on the electronic stopping power of the ions. For ions with low stopping power ($dE/dx_e \leq 17$ MeV mg^{-1}cm^2), the consequence of the irradiation cannot be detected. The AFM image of irradiated mica is very similar to that obtained on virgin mica. In fact, we estimate that defects with a size smaller than the lattice parameter (0.52 nm) cannot be identified in these images. For Kr ions with higher dE/dx_e, AFM images show circular hollows as seen in Fig. 1. Since these hollows were not observed on virgin mica, these defects are identified as the signature of the latent tracks in the cleavage plane of mica. Moreover, their density measured on several large areas on each sample does not vary with dE/dx_e within the measurement accuracy and corresponds to the fluence of the Kr beam (10^{11} ions/cm^2).

As pointed out before, relief in the AFM image may correspond to the real topography and/or to local stiffness changes. In order to clarify the topography of these hollows, AFM images of the same area were recorded for two values of the applied force. As seen in Fig. 2, both the diameter and the depth of the hollow decrease when the applied force is divided by about 2. Such a behavior clearly shows that hollows are not topographic but result from softer areas in the mica surface. A detailed examination of the track image, shown in Fig. 3, reveals that the mica lattice could be recognized in the hollow verge. However, the absence of periodic arrangement is always observed in the inner part of the track. In the particular case of the hollow imaged in Fig. 3, the ratio of the diameter of the hollow to that of the amorphous core attains 1.5.

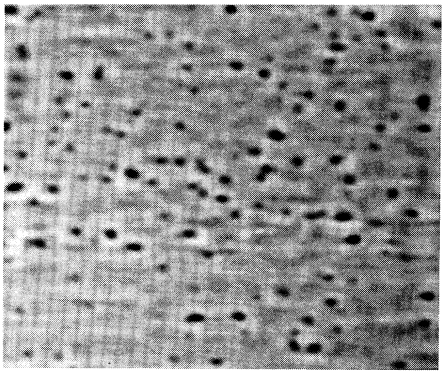

FIG. 1. AFM image of a mica surface irradiated by Kr ions with a stopping power equal to 40 MeV mg^{-1}cm^2. The image size is 400×400 nm^2.

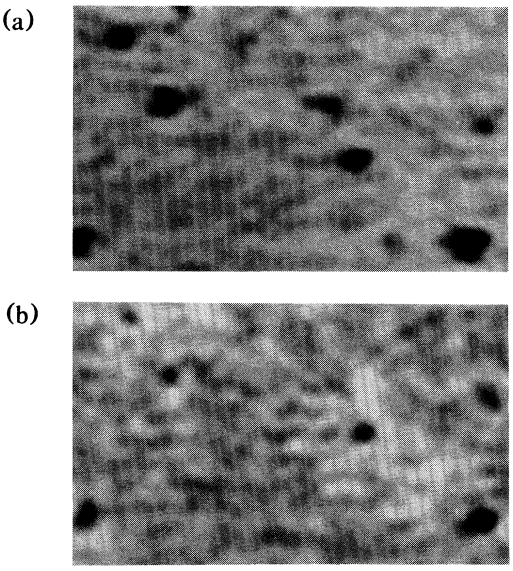

FIG. 2. AFM image of the same area (75×50 nm^2) with two forces: (a) $F\sim9\times10^{-8}$ N; (b) $F\sim5\times10^{-8}$ N. As changes of the applied force modify the hollow geometry, we conclude that the hollow corresponds to a softer area in the surface.

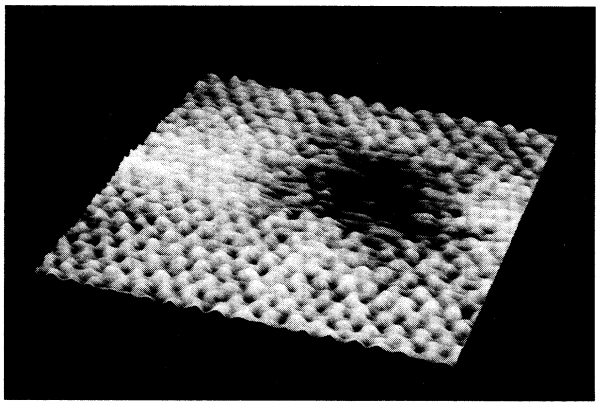

FIG. 3. Detailed 3D view of a hollow (10×10 nm^2). The arrangement of bumps forms a hexagonal lattice on the flat part of the surface. The lattice can be recognized in the verge but not in the inner part of the hollow. The black to white scale corresponds to 1 nm.

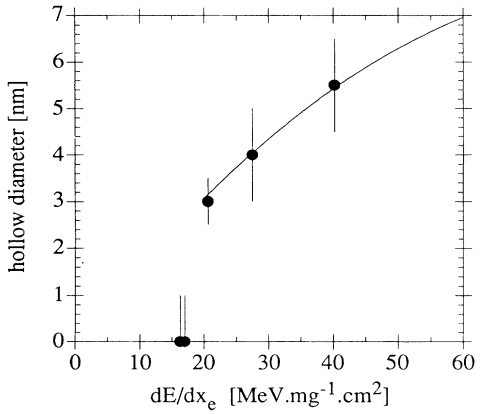

FIG. 4. Mean diameter of hollows as a function of the electronic stopping power of Kr ions (circles). The line corresponds to small-angle scattering measurements [9,10].

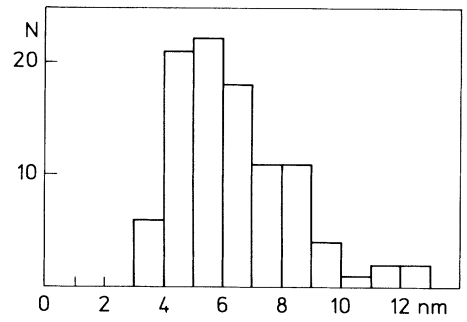

FIG. 5. Histogram of 120 hollow diameters observed on a 400×400-nm^2 image. Hollows with a diameter larger than 11 nm may result from track overlapping.

Observations of hollows on several mica sheets, corresponding to different electronic stopping powers, show that the hollow diameter increases with increasing dE/dx_e. Figure 4 shows the variation of the mean diameter deduced from at least fifty measurements for each dE/dx_e. The same plot reports the data for the mean diameter of the atomic density deficit obtained by small-angle scattering [9,10]. The values are in close agreement with the hollow diameter obtained with applied forces roughly equal to 5×10^{-8} N. It has been noticed that the amorphous core is significantly smaller than the hollow diameter. This comparison suggests that the still crystalline zone surrounding the amorphous core contains a significant concentration of point defects which changes the atomic density and softens the lattice. For a given applied force, the depth of the hollow is then related to the density of defects.

One has to note that, for a given applied force, the hollow sizes show a slight dispersion (Fig. 1). The histogram of the measurement of about 100 hollow diameters is reported in Fig. 5. This dispersion in size could originate from the overlapping of two distinct tracks or from fluctuations in track diameter along one ion path. For the fluence we used and for a mean diameter of 5.5 nm, 91% of the tracks do not overlap. The overlapping cannot quantitatively explain the histogram. The energy loss of a monoenergetic beam of charged particles corresponds to the averaging over a series of single-energy-loss events. The energy loss varies from one point to another and consequently fluctuations in the defect density and in the radii of the damage zone are expected. Moreover, it has been demonstrated that extended defects are only created when the electronic energy loss exceeds a given threshold value [14]. Thus, on account of fluctuations, the local deposited energy could randomly decrease below this threshold, inducing a discontinuity on the track. These discontinuous tracks should be seen on the plane section observed by AFM as a reduction of the measured fluence. Between 20 and 40 MeV mg^{-1}cm^2, the measured fluence is constant within the error bars and the histograms show that the minimum diameters are larger than the detection resolution. So we can conclude that the tracks are constituted by almost continuous disordered zones along the ion paths, but they display some local fluctuations of diameter. Such a description could not be explained by a percolation model with one-radius disordered spheres [15].

In conclusion, we have shown that the hollows observed by AFM in irradiated mica surfaces correspond to softer areas and are associated with the latent track. The core of the tracks is formed by disordered mica. The mean diameter of the observed hollows increases along with the electronic stopping power of the ions. The analysis of the number per unit area and of the diameter distribution of a large number of tracks in a section perpendicular to ion paths allows a description of the track aspect along the ion path. This description is more precise and direct than those issued from other techniques used up to now. For mica, the tracks are nearly cylinder shaped with small modulations of the diameter when dE/dx_e increases from 20 to 40 MeV mg^{-1}cm^2. These observations demonstrate that AFM is indeed a powerful tool for studying local changes of elasticity in materials, such as those induced by swift ions.

We gratefully thank M. Roulliay and M. Drifford for making their AFM available to us. We would like to acknowledge D. Sevin for software support in the image processing. We are indebted to J. C. Jousset and C. Boiziau for having initiated this study.

[1] R. M. Feenstra and G. S. Oehrlein, Appl. Phys. Lett. **47**, 97 (1985).

[2] L. Porte, M. Phaner, C. H. de Villeneuve, N. Moncoffre, and J. Tousset, Nucl. Instrum. Methods Phys. Res., Sect. B **44**, 116 (1989).

[3] R. Coratger, A. Claverie, F. Ajustron, and J. Beauvillain, Surf. Sci. **227**, 7 (1990).

[4] S. A. Durani and R. K. Bull, *Solid State Nuclear Track Detection* (Pergamon, New York, 1987), Chap. 3, p. 23.
[5] M. Toulemonde, G. Fuchs, N. Nguyen, F. Studer, and D. Groult, Phys. Rev. B **35**, 6560 (1987).
[6] M. Toulemonde and F. Studer, Philos. Mag. A **58**, 799 (1988).
[7] R. Katz and E. J. Kobetich, Phys. Rev. **170**, 401 (1968).
[8] H. A. Khan, Nucl. Tracks **12**, 337 (1986).
[9] D. Albrecht, P. Armbruster, R. Spohr, M. Roth, K. Schaupert, and H. Stuhrmann, Appl. Phys. A **37**, 37 (1985).
[10] R. Spohr, P. Armbruster, and K. Schaupert, Radiat. Eff. Defects Solids **110**, 27 (1989).
[11] G. Binning, C. F. Quate, and Ch. Gerber, Phys. Rev. Lett. **56**, 930 (1986).
[12] Digital Instruments.
[13] A. L. Weisenhorn, M. Egger, F. Ohnesorge, S. A. C. Grould, S. P. Heyn, H. G. Hansma, R. L. Sinsheimer, H. E. Gaub, and P. K. Hansma, Langmuir **7**, 8 (1991).
[14] F. Studer, D. Groult, N. Nguyen, and M. Toulemonde, Nucl. Instrum. Methods Phys. Res., Sect. B **19/20**, 856 (1987).
[15] E. Dartyge and P. Sigmund, Phys. Rev. B **32**, 5429 (1985).

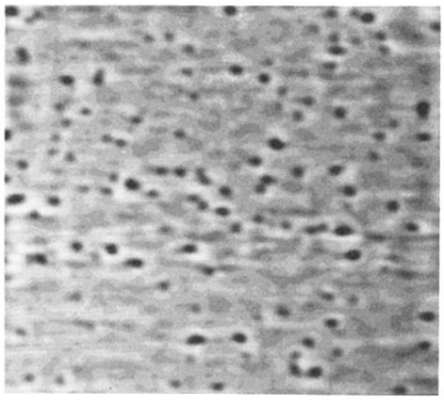

FIG. 1. AFM image of a mica surface irradiated by Kr ions with a stopping power equal to 40 MeV $mg^{-1}cm^2$. The image size is 400×400 nm^2.

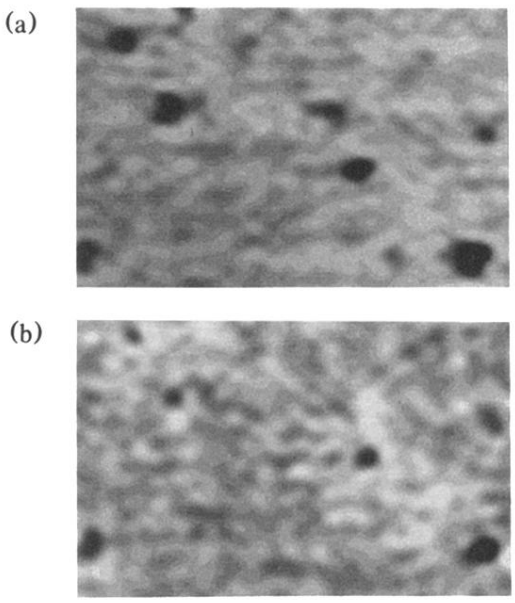

FIG. 2. AFM image of the same area (75×50 nm^2) with two forces: (a) $F\sim9\times10^{-8}$ N; (b) $F\sim5\times10^{-8}$ N. As changes of the applied force modify the hollow geometry, we conclude that the hollow corresponds to a softer area in the surface.

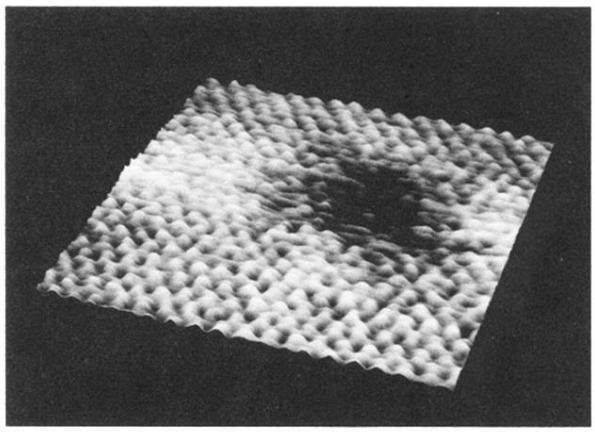

FIG. 3. Detailed 3D view of a hollow (10×10 nm^2). The arrangement of bumps forms a hexagonal lattice on the flat part of the surface. The lattice can be recognized in the verge but not in the inner part of the hollow. The black to white scale corresponds to 1 nm.